

MEMS-based Ethanol Sensor Using Zinc Oxide Nanostructured Films

Hardik Jeetendra Pandya, Sudhir Chandra, Anoop Lal Vyas

Indian Institute of Technology Delhi, Hauz Khas

New Delhi, India

hjpele@yahoo.com, schandra@care.iitd.ernet.in, alvyas@iddc.iitd.ac.in

Abstract—An ethanol sensor incorporating nanostructured zinc oxide film and silicon micromachining is reported. A salient feature of the sensor is its lower operating temperature which has been achieved due to the use of nanostructured material as sensing layer. A suitably designed nickel microheater has been integrated with the sensor. The optimum temperature of operation for ethanol sensing was found to be 100 °C, though the sensor could operate at temperature as low as 50 °C with reduced sensitivity. The power consumption, at an operating temperature of 100 °C, was 180 mW while at 50 °C, it is only 90 mW. The sensor is capable of giving detectable response for concentrations of ethanol vapor as low as 10 ppm.

Keywords- Zinc films; Zinc oxide nanocombs; Thermal evaporation; Lithography; Ethanol sensor.

I. INTRODUCTION

Sensors based on metal oxides for detection of volatile organic compounds (VOCs) and gases have been widely investigated because of their small size, low cost and compatibility with semiconductor processing. ZnO has great potential for use in gas sensors because of the high mobility of conduction electrons and good chemical and thermal stability under the operating conditions. The higher operating temperature (approximately 400 °C) and poor sensitivity are some of the major concerns in using ZnO as sensing layer [1]. The use of CMOS (complimentary metal oxide semiconductor) compatible MEMS (micro-electro-mechanical-systems) technologies in sensor fabrication is advantageous on account of miniaturization of the devices, lower power consumption, faster sensor response, batch fabrication at reduced cost and greater sensitivity [2–5].

The use of nano-structured materials for the sensing device is envisaged to further improve the sensitivity of these devices. This is attributed to enormously increased surface to volume ratio compared to their bulk counterpart. It is further envisaged that the use of nanostructured material may leads to lowering of operating temperature of gas sensors based on metal oxide semiconductors [6]. Very few reports have been published on sensors using nano-structured ZnO thin film on micromachined silicon substrate [8, 9]. In most of the publications on sensors incorporating micromachined microheaters, either platinum or polysilicon microheater has been used as the heating element as these materials are particularly suitable for the

higher temperature operation (400–700 °C) [10–12]. Furthermore, with a view to reduce the power consumption, the platforms for micromachined gas sensor reported so far are based on a SiO₂-Si₃N₄ composite layer on a thick (~ 400 μm) silicon substrate [13]. A thin Si plug underneath the dielectric membrane can be used for achieving uniform temperature distribution over the active heater area owing to the higher thermal conductivity of Si [14]. Recently, few reports on operating gas sensors at relatively lower temperatures using nanotextured semiconducting oxides have been published [7, 15]. This type of gas sensor operates at relatively lower temperature (150–250 °C) and does not require an expensive Pt or poly-Si microheater [7, 15]. The microheater may be fabricated using a low cost material such as nickel.

The present work is an attempt to address the problems of elevated operating temperature and high power consumption by taking a twin approach namely: (a) reducing the operating temperature through the use of nanostructured metal oxide (ZnO) and (b) reducing the power consumption through the deployment of MEMS structure with a thin silicon membrane. In this paper we report a nanostructured ZnO based sensor using micromachined silicon substrate for efficient detection of ethanol vapors in the range of 200 – 1000 ppm at fairly low operating temperature of 50 °C. For this purpose, a nickel microheater has been designed and monolithically integrated with the sensor to obtain the required heating of the sensing layer. The response of the nanostructured ZnO based sensor having an integrated nickel microheater has been evaluated at different operating temperatures in the range of 30–100 °C, for different concentrations of ethanol vapors.

II. EXPERIMENTAL WORK

A schematic drawing of the sensor structure is shown in Fig. 1 and the corresponding process flowchart is shown in Fig. 2. The starting silicon wafer is 280 μm thick, N-type, having 5-10 Ω-cm resistivity and (100) orientation. A layer of SiO₂ (0.8 μm) was grown by thermal oxidation process. After opening a window in SiO₂ by photolithography technique on the backside of the wafer, bulk micromachining was carried out in 40 % KOH solution at a temperature of 80 °C, to obtain a 100 μm Si membrane.

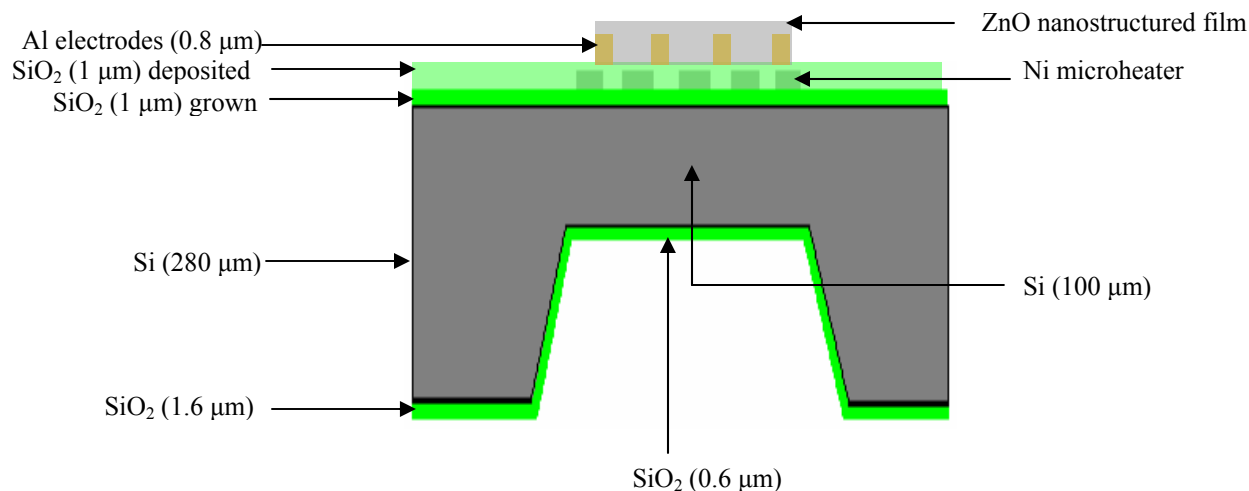


Figure 1. A schematic diagram of the MEMS gas sensor.

A silicon oxide layer (0.8 μm) was then grown in the next step. The purpose of this oxidation is to reduce the thermal losses from the backside of the membrane. A layer of nickel (0.3 μm thickness) was then deposited using RF diode sputtering on the front side of the oxidized wafer. The Ni layer was then patterned using photolithography to form the microheater. The meander shaped Ni microheater has line- width of 100 μm and the gap between the lines was also kept 100 μm. A layer of SiO₂ (0.8 μm) was then sputter deposited on the front side of the wafer. The purpose of this step is to electrically isolate the heater and the aluminum interdigital electrodes (to be formed in the next step). The aluminum layer of 0.8 μm was then deposited by thermal evaporation and patterned to form the sensing interdigital electrodes. A thin film of Zn (0.3 μm) was then deposited by thermal evaporation and patterned using photolithography process. The wafer was then heated to 300 °C in air for 6 h and cooled slowly to room temperature. It was observed that, following the annealing process, the color of the deposited Zn films turned white from the grey color of the as-deposited zinc films. The active area of the sensing layer was 2 mm X 2 mm while the total chip size was 5 mm X 5 mm.

III RESULTS AND DISCUSSION

The SEM image of the backside of the membrane is shown in the Fig. 3. Most of the papers reported so far use a freestanding dielectric layer (SiO₂ or SiO₂-Si₃N₄ composite) for lower power consumption and higher operating temperature at the cost of long-term stability [16-17]. In the present work, a 100 μm Si membrane has been used for better mechanical stability which also provides fairly good temperature uniformity. The SEM image of Ni microheater is shown in Fig. 4. The resistance of the heater was measured to be about 120 Ω. The experimentally

measured power consumption versus temperature graph for the Ni microheater is shown in Fig. 5.

It can be observed that the power consumption, at a temperature of 50 °C, was 90 mW and at 100 °C, it was 180 mW. The microheater was driven by 5 V supply. The X-ray diffractograms (XRD) of the as-deposited Zn film and ZnO film (obtained by annealing of Zn film in air at 300 °C for 6 h) are shown in Fig. 6. The XRD of the annealed film shows the peaks corresponding to ZnO, confirming that the Zn film has been completely oxidized to form ZnO. The SEM image of nanostructured ZnO film is shown in Fig.7. It can be seen that the film consists of nanocombs of ZnO. It is further observed that each comb is composed of stem to which many nanowires are attached. The nanowires have diameter in the range 40-50 nm and length of up to 500 nm.

The sensor was tested for ethanol vapors in a closed chamber. The sensor was heated to different temperatures by applying power to the integrated heater. The ethanol vapors were introduced in the chamber by bubbling N₂ through the ethanol maintained at room temperature (20 °C). The desired concentration of the vapors was obtained in the chamber by controlling the flow rate of N₂ through ethanol and adding pure air through a separate gas line [18]. The flow rates were measured and controlled using precession flow meters. The concentration of ethanol vapors was calculated using the following equation [19].

$$C = \frac{\frac{P^* \times L}{760 - L}}{\frac{P^* \times L}{760 - L} + L + L^*} \times 10^6 \quad (1)$$

where, L and L* are gas flow rates of N₂ (through the bubbler) and air respectively. P* is the vapor pressure of the ethanol (in mm of Hg) at room temperature (20 °C).

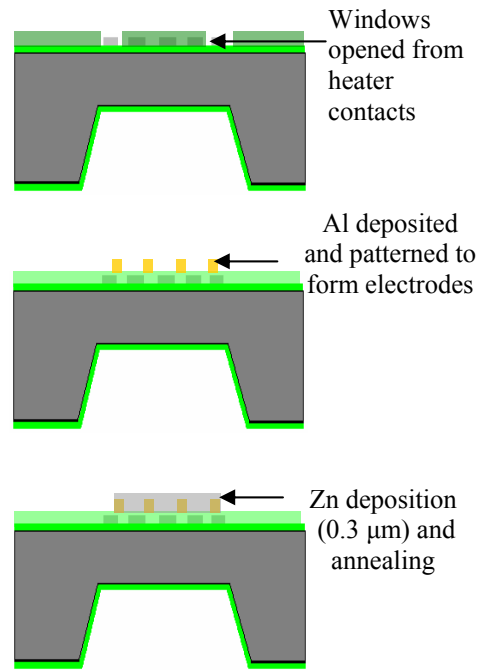
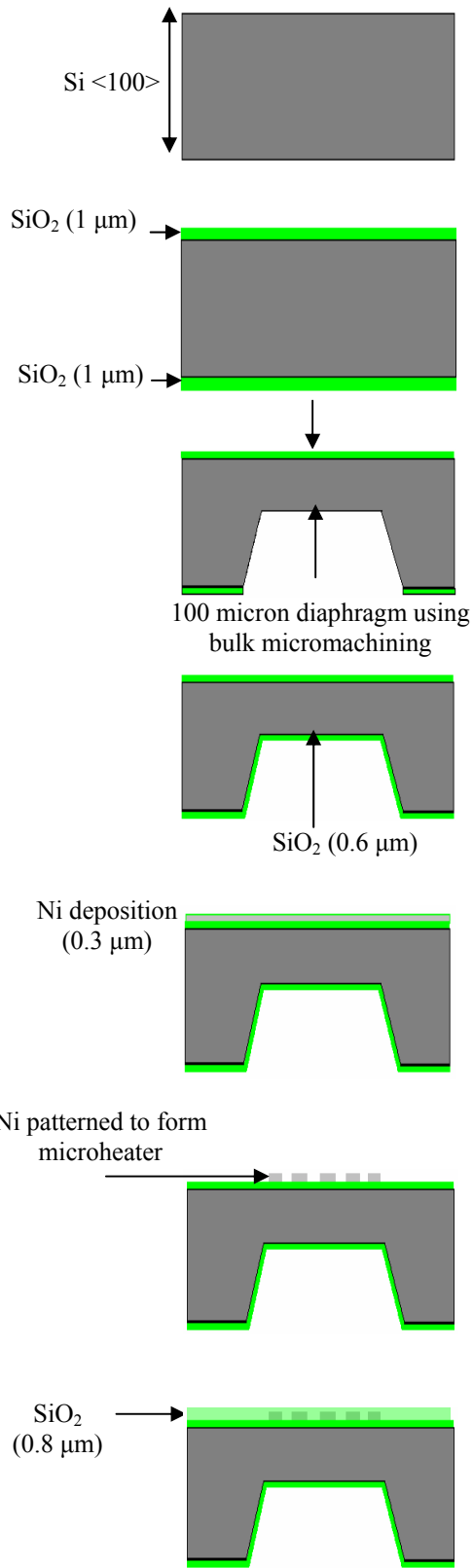


Figure 2. Process flow chart for the fabrication of nanostructured ZnO based micromachined ethanol sensor with embedded Ni microheater.

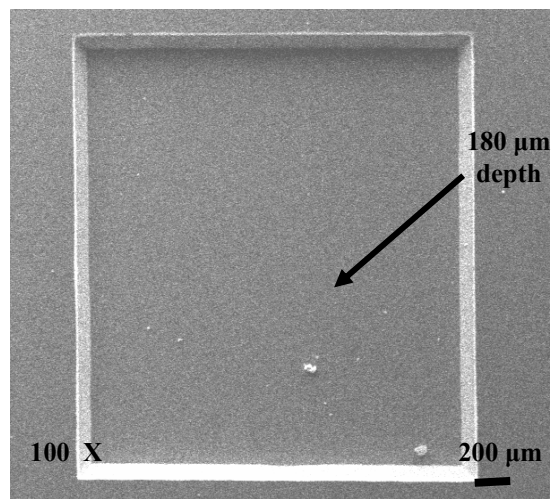


Figure 3. SEM image of micromachined diaphragm from the back side.

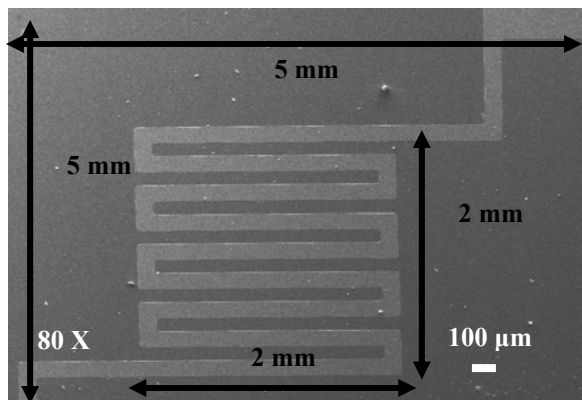


Figure 4. SEM image of nickel microheater

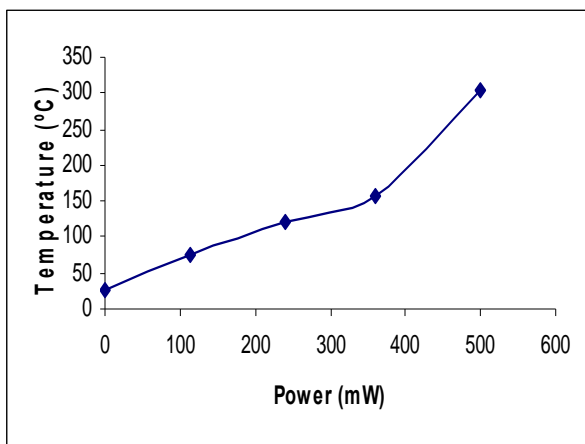


Figure 5. Plot of power versus temperature obtained for Ni microheater

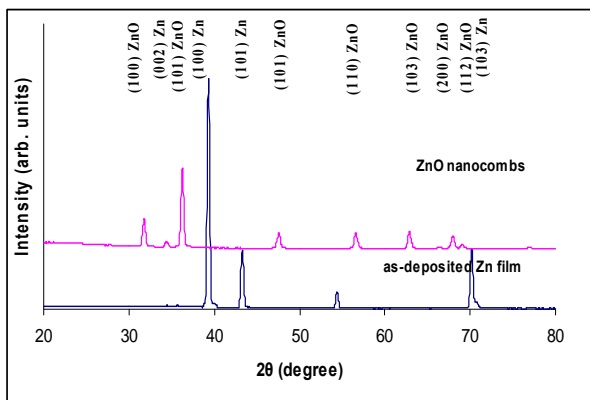


Figure 6. XRD micrographs of as-deposited Zn film and Zn annealed at 300 °C for 6 h.

Based on this equation, the relationship between the flow rates and the concentration of ethanol in ppm is summarized in Table 1. Fig. 8 shows the response $(R_a - R_g) / R_g$ of the

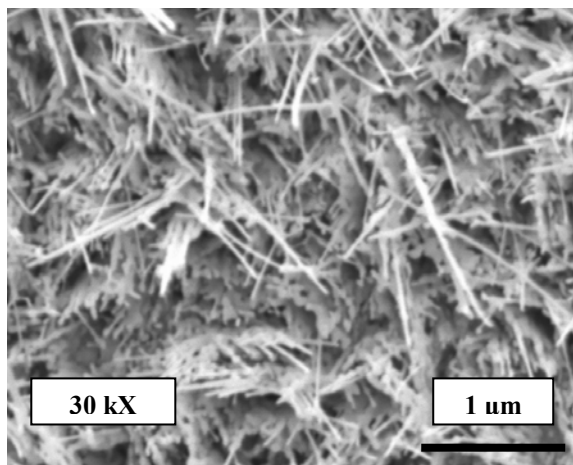


Figure 7. SEM image of ZnO nanocombs obtained after annealing Zn film (300 nm) at 300 °C for 6 h.

sensor for 200 ppm of ethanol vapors as a function of its operating temperature. Here, we define R_a and R_g as the resistance of the sensor in clean air and in the ethanol containing air respectively. From Fig. 8, it can be observed that the maximum sensitivity is achieved at the operating temperature of 100 °C. At the lowest operating temperature of 30 °C, the sensitivity falls significantly, but the sensor is still able to detect the presence of ethanol.

Table I. Relationship between flow rates and ethanol vapor concentrations in the test chamber at 20 °C. The vapor pressure (P^*) of ethanol at 20 °C is 67.5 mm of Hg [19, 20].

Flow rate of N_2 through bubbler containing ethanol (ml/min)	Flow rate of air used for diluting ethanol concentration (L/min)	Ethanol concentration (ppm)
10	5	180
20	5	363
20	4	453
30	5	552
40	5	746
50	5	940

At 50 °C, the sensitivity of the sensor improves significantly. It is evident from Fig. 8 that as the operating temperature of the sensor decreases the time to reach the saturation level increases. This is consistent with the operation of gas sensors based on metal oxides [9, 12]. Fig. 9 shows the response of the sensor to successively increasing concentrations of ethanol vapor. This was achieved by increasing the flow rate of N_2 through the bubbler corresponding to the desired concentration levels, as shown in Table 1. As expected, the sensitivity increases for higher concentrations of ethanol. Furthermore, it can be

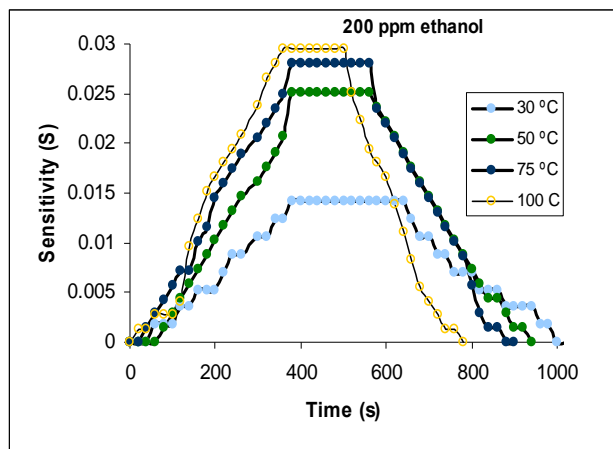


Figure 8. Response of sensor to 200 ppm of ethanol vapors as a function of operating temperature.

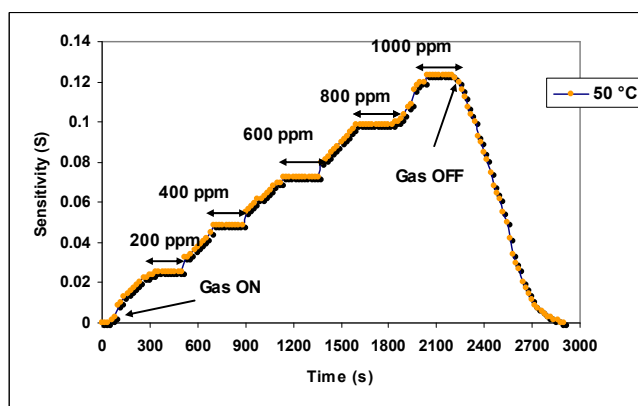


Figure 9. The dynamic response of the sensor for different concentration of ethanol vapors on injection and switching off the N_2 passing through bubbler.

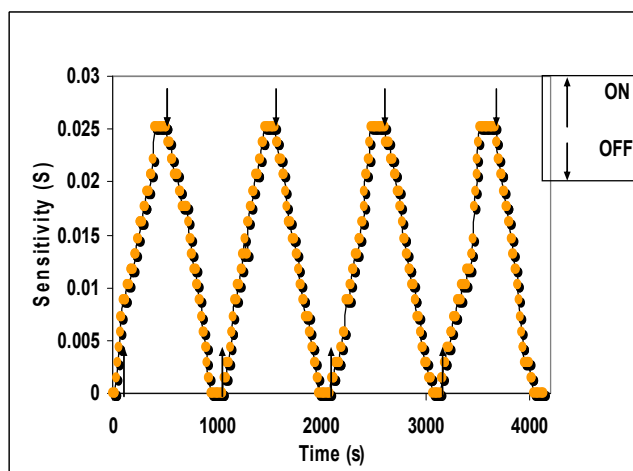


Figure 10. Dynamic response of the sensor for 200 ppm ethanol vapor operating at 50 °C. The arrows indicate the switching ON and OFF of N_2 flowing through the bubbler containing ethanol.

seen that there is varying delay in reaching the saturation value of the sensor resistance, as the ethanol concentration is increased in steps. Since the volume of the test chamber is quite large (14 L) in our test set up, this does not reflect the true response time of the sensor [18]. The dynamic response of the sensor was also evaluated. For this purpose, the N_2 gas (flowing through the bubbler) was turned ON and OFF periodically, as indicated in Fig. 10. Measurements were made at an operating temperature of 50 °C. It is evident that the response of the sensor is reproducible for the selected concentration of ethanol vapors (200 ppm). The response and recovery time of the sensor was almost constant for several cycles which show the good repeatability of the sensor. It was also found that the sensor is sensitive to humidity. Furthermore, if more than one VOC vapors are present then the sensor may give false response.

CONCLUSION

We have successfully synthesized nanostructured ZnO by a low cost process of oxidation of Zn film in air without using any template or catalyst. The integration of the nanostructured ZnO with sensor fabrication process is demonstrated. The sensitivity of the sensor is significantly enhanced and the operating temperature is considerably reduced by using the ZnO nanostructured material. Lowering of the operating temperature of the sensor has significant advantage in terms of power consumption and choice of the heater material. A low cost nickel heater has been successfully integrated with the sensor in the present work. ZnO based MEMS micro-hotplate (with Ni microheater) provides a promising platform for low power sensors for ethanol sensing at a fairly low operating temperature of 50 °C. Integration of nanostructure ZnO film along with MEMS technology provides a platform for low power low temperature sensor with appreciable sensitivity and response time. It will be interesting to see the sensor behavior in the presence of other VOCs.

REFERENCES

- [1] B.L. Zhu, C.S. Xie, W.Y. Wang, K.J. Huang, and J.H. Hu, "Improvement in gas sensitivity of ZnO thick film to volatile organic compounds (VOCs) by adding TiO_2 ", Mater. Lett. 58, pp. 624-629, 2004.
- [2] K.D. Mitzner, J. Strnhagen, and D.N. Glipeau, "Development of micromachined hazardous gas sensor array", Sensors Actuators B, 93, pp. 92-99, 2003.
- [3] J.S. Suehle, R.E. Cavicchi, M. Gaitan, and S. Semancik, "Tin oxide gas sensor fabricated using CMOS micro-hotplates and in situ processing", IEEE Electron Dev Lett, 14(3), pp. 118-120, 1993.
- [4] J.A. Salcedo, J.L. Juin, Y.M. Afridi, and R.A. Hefner, "On-chip electrostatic discharge protection for CMOS gas sensor systems-on-a-chip (SoC)", Microelectron Reliab, 46, pp. 1285-1294, 2006.

- [5] X. Lafontan, F. Pressecq, F. Beaudoin, S. Rigo, M. Dardalhon, and J.L. Roux, "The advent of MEMS in space", *Microelectron Reliab.*, 43(7), pp. 1061–1083, 2003.
- [6] E. Comini, G. Faglia, G. Sberveglieri, Z. Pan, and Z.L. Wag, "Stable and highly sensitive gas sensors based on semiconducting oxide nanobelts", *Appl Phys Lett*, 81, pp. 1869–1871, 2002.
- [7] P. Bhattacharyya, P.K. Basu, H. Saha, and S. Basu, "Fast response methane sensor using nanocrystalline zinc oxide thin films derived by sol–gel method", *Sensors Actuators*, B124, pp. 62–67, 2004.
- [8] F. Hassani, O. Tigli, S. Ahmadi, C. Korman, and Zaghoul, "Integrated CMOS surface acoustic wave gas sensor: design and characteristics", *Proc IEEE Sensors*, 2, pp. 1199–1202, 2002.
- [9] Q. Wan, Q.H. Li, Y.J. Chen, T.H. Wang, X.L. He, and J. P. Li, "Fabrication and ethanol sensing characteristics of ZnO nanowire gas sensors", *Appl Phys Lett*, 84, pp. 3654–3656, 2004.
- [10] S.M. Lee, D.C. Dyer, and J.W. Gardner, "Design and optimization of a high-temperature silicon micro-hotplate for nanoporous palladium pellistors", *Microelectron Journal*, 43, pp. 115–1126, 2003.
- [11] J. Puigrobo, D. Vogel, B. Michel, A. Vila, I. GraciaI, and C. Cane, "Thermal and mechanical analysis of micromachined gas sensors", *J Micromech Microeng*, 13, pp. 548–556, 2003.
- [12] W. Chung, C. Shim, S. Choi, and D. Lee, "Tin oxide microsensor for LPG monitoring", *Sensors Actuators*, B20, pp. 139–43, 1994.
- [13] C. Rossi, E. Scheid, and D. Esteve, "Theoretical and experimental study of silicon micromachined microheater with dielectric stacked membranes", *Sensors Actuators*, A63, pp. 183–189, 1997.
- [14] A. Gotz, I. GraciaI, C. Cane, E. Lora-Tamayo, M.C. Horrilo, and J. Getino, "A micromachined solid state integrated gas sensor for the detection of aromatic hydrocarbons", *Sensors Actuators*, B44, pp. 483–487, 1997.
- [15] P. Nunes, E. Fortunato, A. Lopes, and R. Martins, "Influence of the deposition conditions on the gas sensitivity of zinc oxide thin films deposited by spray pyrolysis", *Int J Inorg Mater*, 3, pp. 1129–1131, 2001.
- [16] L.Y. Sheng, Z. Tang, J.P. Wu, C.H. Chan, and J.K.O. Sin, "A low-power CMOS compatible integrated gas sensor using maskless tin oxide sputtering", *Sensors Actuators*, B49, pp. 81–87, 1998.
- [17] C. Rossi, P.T. Boyer, and D. Esteve, "Realization and performance of thin SiO₂/Si₃N₄ membrane for microheater applications", *Sensors Actuators*, A 64, pp. 241–245, 1998.
- [18] H.J. Pandya, Sudhir Chandra, and A.L.Vyas, "Fabrication and characterization of ethanol sensor based on RF sputtered ITO films", *Sensors and Transducers*, 10, pp. 141-150, 2011.
- [19] C.B. Lim, J.B. Yu, D.Y. Kim, H.G. Byun, D.D. Lee, and J.S. Huh, "Sensing characteristics of nano-network structure of polypyrrole for volatile organic compounds (VOCs) gases", *IEEE Sensors*, pp. 695-698, 2006.
- [20] H. Das, "Food Processing Operation Analysis", Asian Books Private Limited, 2005.